Aerospace Science and Technology ••• (••••) •••–•••

Contents lists available at SciVerse ScienceDirect

Aerospace Science and Technology

www.elsevier.com/locate/aescte

Prediction of icing effects on the lateral/directional stability and control of light airplanes

Amanda Lampton [1], John Valasek [*,2]

Texas A&M University, College Station, TX 77843-3141, United States

ARTICLE INFO

Article history:
Received 11 February 2008
Received in revised form 26 July 2011
Accepted 22 August 2011
Available online xxxx

Mots-clés :
Six degree-of-freedom simulation
Stability derivatives
Modeling of icing effects
Distributed icing
Icing severity
Sensitivity to pilot input

ABSTRACT

The accumulation of ice on an airplane in flight is one of the leading contributing factors to general aviation accidents, and to date only relatively sophisticated methods based on detailed empirical data and flight data exist for its analysis. This paper develops a methodology and simulation tool for a preliminary yet accurate evaluation of airplane dynamical response and stability and control characteristics due to icing. It uses only basic mass properties, configuration, and propulsion data, together with known icing data obtained for similar configurations. Existing icing data for a light airplane is suitably modified and applied to a non-real-time, six degree-of-freedom simulation model of a different but similar light airplane, developed from empirical data and Data Compendium methods. The component build-up method is used to implement icing effects on the wing alone, horizontal tail alone, and various unequal distributions of combined wing and horizontal tail icing as well as ice accretion on only one half of the wing. Results presented in the paper are limited to the roll axis and yaw axis maneuvers with various levels and distributions of ice accretion show that the methodology captures the basic detrimental effects of ice accretion on roll and yaw response and lateral stability, in addition to the sensitivity of pilot control response.

© 2011 Elsevier Masson SAS. All rights reserved.

1. Introduction

Rime, glaze, and mixed ice along the leading edge of lifting surfaces all have detrimental effects on aircraft performance. Although anti-icing devices such as de-icing boots and heating strips help, ice accretions can still build up and affect the aircraft adversely by decreasing static lateral stability, especially in the case when the aircraft does not develop ice accretions evenly between wing halves. Additionally, malfunctions of these anti-icing systems can result in ice buildup aft of the devices themselves, or ice buildup between the cycles of the de-icing systems.

The danger of a lateral maneuver with ice accretions on the aircraft lays in the susceptibility of the ice causing a separation bubble [10]. This phenomenon is usually caused by a horn of ice disrupting the flow of air over the airfoil and creating an adverse pressure gradient. This disruption forms a separation bubble that reattaches further downstream. However, increasing the aileron deflection angle increases the relative angle-of-attack over the wing as the aircraft rolling moment increases, thus pushing the reattachment point farther downstream and increasing the size of the separation bubble [3]. As the bubble increases in size, aileron and rudder effectiveness decreases and full departure of the aircraft becomes more likely. The effect of full tail icing has been shown to decrease weathercock stability, C_{n_β}, as well as reduce rudder effectiveness [18]. Bragg et al. have developed an icing effects model applicable to any performance, stability, or control derivative affected by icing [4]. The model is characterized by dependence on atmospheric conditions, susceptibility of an aircraft to icing, and a given derivative as seen in Eq. (1).

$$C_{(A)_{iced}} = \left(1 + \eta_{ice} k'_{C_A}\right) C_{(A)} \tag{1}$$

This model is still being refined, with many of the influencing factors still unknown [4]. The model was then integrated into a Flight Dynamics and Control toolbox for MATLAB and SIMULINK [19], which produces results showing the possible changes of an airplane's stability derivatives over time with icing effects.

The practicality of using an autopilot during icing conditions has also been studied. Sharma et al. have designed a pitch angle hold autopilot that considers ice accretion severity when processing the commanded pitch attitude angle; the goal being to maintain the stability of the airplane [21]. The issue of distributed icing levels and sensitivity to pilot input is not addressed. The research described in Ref. [22] concerns the dangerous reduction in stall angle-of-attack and how climbing at high angles-of-attack could

* Corresponding author.
E-mail addresses: alampton@tamu.edu (A. Lampton), valasek@tamu.edu (J. Valasek).
[1] Graduate Research Assistant, Flight Simulation Laboratory, Aerospace Engineering Department, Student Member AIAA.
[2] Associate Professor and Director, Flight Simulation Laboratory, Aerospace Engineering Department, Associate Fellow AIAA.

1270-9638/$ – see front matter © 2011 Elsevier Masson SAS. All rights reserved.
doi:10.1016/j.ast.2011.08.005

Please cite this article in press as: A. Lampton, J. Valasek, Prediction of icing effects on the lateral/directional stability and control of light airplanes, Aerospace Science and Technology (2011), doi:10.1016/j.ast.2011.08.005

approach this reduced stall angle causing an unexpected wing stall. Ref. [20] employs Navier–Stokes analysis to test the flowfield and resulting lift and drag produced by a wing section with various ice shapes. The most significant finding is that 5 minute ice accretions were found to produce severe lift and drag degradation. Much other research in the area of the influence of ice regards airfoil aerodynamics. In general, the consensus appears to be that the aerodynamics of an airfoil is degraded by ice accretion such that lift decreases, drag increases, stall angle-of-attack is reduced, and pitching moment is degraded [3,7–9,14–16,22,23]. Efforts have been made to develop icing protection systems, especially Bragg et al. They propose a smart icing system based on the ability to sense the effect of ice on aircraft performance, stability, and control [6]. Ref. [17] develops a method to monitor inflight ice accretion effects using parameter identification.

Airplane response due to pilot command inputs with the autopilot disengaged is a critical safety issue, since the FAA recommends that the autopilot must be disengaged during flight in known icing conditions. The danger lies in a pilot attempting to command an iced airplane in the same way as a non-iced airplane, since overly aggressive pilot command inputs (for the iced situation) can produce an unexpected response due to performance degradation, which can lead to stall, overshoots and undershoots in commanded altitude, and excessive rolling and pitching moments. This is particularly critical for situations in which the pilot is not even aware that the airplane response and performance has been compromised by icing, and it has not been reported on in the open literature.

In Ref. [13], the authors developed a simplified method for the prediction of icing effects and pilot command effects on the dynamic response, stability, and climb performance of light airplanes, for which icing data may not exist or might not be obtainable. It also considers the modeling and evaluation of unequally distributed icing levels & icing severity between the wing, wing halves, the horizontal tail, and the full aircraft, in terms of dynamic response. However, the approach and results were all limited to the pitch axis only, and therefore did not account for the lateral/directional dynamics, or the coupled response between the three axes.

The contribution of this paper is an extension of the methodology presented in Ref. [13]. It is an alternative and simplified method for the prediction of icing effects on the lateral/directional dynamic response and performance of light airplanes. The approach developed here uses known icing data for a given airplane configuration (obtained from either flight data or wind tunnel data or both) and applies it via appropriate scaling and modification to a different airplane of similar configuration. These icing effects are used in a component buildup fashion to develop a linear time invariant (LTI), six degree-of-freedom, non-real-time flight simulation code used for investigating dynamic response, stability, and rolloff tendencies for various levels of ice accretion, and unequal icing distributions between the right and left half of the wing, which can either result when flying in icing conditions with a crosswind or when a deicing boot malfunctions. The utility of this approach is the ability to investigate the dynamic response due to various icing distributions for airplanes for which icing data does not exist. An additional advantage of this approach compared to earlier work in the literature is the ability to evaluate a variety of time-varying pilot inputs, such as singlets, doublets, and ramps. Because of this feature, the important effect of under-commanding or over-commanding an iced airplane during lateral maneuvers can be evaluated. In total, the approach developed in this paper permits a rapid, first cut analysis of icing effects using only basic, relatively easy to obtain or generate data as a prelude to a highly detailed analysis using sophisticated methods. The scope of this paper is limited to the roll axis and yaw axis, where detrimental icing effects can be experienced.

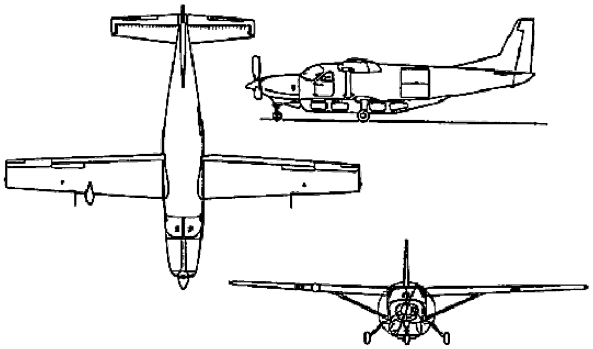

Fig. 1. Cessna 208B Super Cargomaster external characteristics.

The paper is organized as follows. First a non-parametric linear model of a Cessna 208B Super Cargomaster (Fig. 1) is developed, in which stability and control derivatives are calculated using the DATCOM and Advanced Aircraft Analysis (AAA) computer program [1]. Verification of the model is accomplished by comparing simulation data to published data. To ensure the fidelity of the model a modal analysis to examine the characteristics of the flight modes was conducted. In addition, a controllability analysis was conducted to check that the system was indeed linearly independent and controllable. Next, the stability derivatives calculated for each flight condition of interest are used to construct multiple linear time-invariant state-space models used for non-real-time simulation. Various levels of ice accretion severity are then added to the clean aircraft simulation based on icing data gathered by NASA Glenn on the DeHavilland Twin Otter [4]. Finally, numerical examples consisting of either a rudder 3–1–2 followed by an aileron doublet or uneven icing between wing halves with different amounts of ice accretion applied to the aircraft are presented. Finally, a summary and conclusions are presented.

2. State-space model representation

To determine the response of a linear-time-invariant (LTI) system to an arbitrary input signal, it is transformed into a state-space representation of the system. The system analyzed in this paper is a continuous dynamic linear system in the stability axis. Time-invariance of the model is assumed since the parameters in the model do not change quickly for the relatively slow maneuvers examined here. Consider first the linear time-invariant state-space model of perturbations about the steady-state or trim condition

$$\dot{\boldsymbol{X}} = A\boldsymbol{X} + B\boldsymbol{U}$$
$$\boldsymbol{Y} = C\boldsymbol{X} + D\boldsymbol{U} \tag{2}$$

where $\boldsymbol{X} \in \mathbb{R}^{n\times 1}$ is a state vector, $A \in \mathbb{R}^{n\times n}$ is a plant matrix, $\boldsymbol{U} \in \mathbb{R}^{m\times 1}$ is an input vector, $B \in \mathbb{R}^{n\times m}$ is a control distribution matrix, $\boldsymbol{Y} \in \mathbb{R}^{r\times 1}$ is an output vector, and $C \in \mathbb{R}^{r\times n}$ and $D \in \mathbb{R}^{r\times m}$ are matrices that determine the elements of the output vector.

Consider the lateral/directional linear equations of motion of this coupled system in stability-axes defined as Taylor series expansions:

$$\dot{\beta} = \big(Y_p p + g\phi\cos\Theta_1 + Y_\beta\beta + (Y_r - U_1)r + Y_{\delta_A}\delta_A + Y_{\delta_R}\delta_R\big)/U_1$$
$$\dot{p} = L_\beta\beta + L_p p + L_r r + L_{\delta_A}\delta_A + L_{\delta_R}\delta_R + \frac{I_{xz}}{I_{xx}}\dot{r}$$
$$\dot{r} = N_\beta\beta + N_p p + N_r r + N_{\delta_A}\delta_A + N_{\delta_R}\delta_R + \frac{I_{xz}}{I_{zz}}\dot{p}$$

Please cite this article in press as: A. Lampton, J. Valasek, Prediction of icing effects on the lateral/directional stability and control of light airplanes, Aerospace Science and Technology (2011), doi:10.1016/j.ast.2011.08.005

$$\dot{\phi} = p + r\tan\Theta_1$$
$$\dot{\psi} = r\sec\Theta_1 \tag{3}$$

These affine in the control, coupled equations assume steady level 1-g trimmed flight in the stability axis system such that $P_1 = Q_1 = R_1 = V_1 = W_1 = \Phi_1 = 0$, and $\Theta_1 = \text{constant}$. Following a similar derivation as that shown in Refs. [13] and [11], the lateral/direction state-space model is

$$\begin{bmatrix} \dot{\beta} \\ \dot{p} \\ \dot{r} \\ \dot{\phi} \\ \dot{\psi} \end{bmatrix} = \begin{bmatrix} \frac{Y_\beta}{U_1} & \frac{Y_p}{U_1} & (\frac{Y_r}{U_1} - 1) & \frac{g\cos\Theta_1}{U_1} & 0 \\ L'_\beta & L'_p & L'_r & 0 & 0 \\ N'_\beta & N'_p & N'_r & 0 & 0 \\ 0 & 1 & \tan\Theta_1 & 0 & 0 \\ 0 & 0 & \sec\Theta_1 & 0 & 0 \end{bmatrix} \begin{bmatrix} \beta \\ p \\ r \\ \phi \\ \psi \end{bmatrix} + \begin{bmatrix} \frac{Y_{\delta_A}}{U_1} & \frac{Y_{\delta_R}}{U_1} \\ L'_{\delta_A} & L'_{\delta_R} \\ N'_{\delta_A} & N'_{\delta_R} \\ 0 & 0 \\ 0 & 0 \end{bmatrix} \begin{bmatrix} \delta_A \\ \delta_R \end{bmatrix} \tag{4}$$

The elements of Eq. (4) are determined from non-dimensional stability and control derivatives extracted from AAA for a DATCOM model of the Cessna 208B developed using the Maintenance Manual for the airplane [2], and verified by flight test data. AAA is a software code based on the USAF Data Compendium (DATCOM). Major assumptions made in the development of the DATCOM model were i) the exact location of the transition point from laminar to turbulent flow on the lifting surfaces, ii) the drag increment due to gaps between lifting and control surfaces, iii) steady flow, and iv) linear model is accurate up to angular displacements of 15° and velocity perturbations up to 100 ft/s. A universal location of 14% of the chord of the lifting surface is used as the transition point from laminar to turbulent flow. For the drag increment a value of 0.00036 is used. Values of the stability and control derivatives used for calculations in this paper are provided in Appendix A.

Ref. [12] contains the detailed modal analysis that is summarized here. The lateral/directional dynamics consist of the three standard modes, Dutch roll, roll, and spiral. All are stable for the present flight condition. For the Cessna 208B, it was determined that the sideslip angle and the aircraft heading is most affected by the ailerons and rudder, whereas the roll rate is only significantly affected by the ailerons. Yaw rate is affected to a lesser extent by the rudder. The second-order mode (Dutch roll) is made up primarily of yaw rate and to a lesser extent, roll attitude angle. One of the first order modes is composed of sideslip and roll rate, while the other first order mode is composed mainly of roll attitude angle and yaw rate. These modes and their compositions are as expected. A controllability analysis using the controllability grammian verifies that the system is controllable.

3. Simulation development

Consistent with the scope of this work, which is to determine degradation due to ice accretions for several parameters via numerical simulation, the continuous-time LTI model developed above must be discretized. This discrete-time LTI system is defined as

$$\boldsymbol{X}_{k+1} = \Phi\boldsymbol{X}_k + \Gamma\boldsymbol{U}_k$$
$$\boldsymbol{Y}_k = C\boldsymbol{X}_k + D\boldsymbol{U}_k \tag{5}$$

where $\Phi \in \mathbb{R}^{n\times n}$ and $\Gamma \in \mathbb{R}^{n\times m}$ are the state transition matrix and discrete control distribution matrix, respectively, and are dependent on $A \in \mathbb{R}^{n\times n}$, $B \in \mathbb{R}^{n\times m}$, and h, the time step of the discrete-time model. Φ and Γ of the discrete model are related to their continuous model counterparts, A and B, by the following equations:

$$\Phi(h) = e^{Ah} \tag{6}$$

$$\Gamma = \left(\int_0^h e^{A\tau}\,d\tau\right)B \tag{7}$$

The simulation is coded using MATLAB 7.1. By loading values determined from AAA for a given flight condition into the LTI state-space model in MATLAB, the discretized model can be determined using commands imbedded in the program. This is done for both a clean airplane and an iced airplane.

4. Modeling and incorporation of icing effects

The extent to which each stability and control derivative is affected by ice accretions is based on previous studies, in particular those concerning the flight dynamics of a DeHavilland Twin Otter [4,23]. Twin Otter data was used because there is more icing data available of the type needed for this research than for any other aircraft reported in the open literature. In general, the effectiveness of C_{Y_β}, $C_{Y_{\delta_r}}$, C_{l_β}, C_{l_p}, $C_{l_{\delta_a}}$, $C_{l_{\delta_r}}$, C_{n_β}, C_{n_r}, and $C_{n_{\delta_r}}$ has been observed to degrade between 5% and 25%. As ice builds up on the leading edge of the wing, horizontal tail, and vertical tail, the carefully engineered surfaces are compromised. Thus they produce less lift. Also, the ice accretion may develop horns that protrude into the airflow as well as increasing surface roughness leading to an increase in drag. These changes in lift and drag contribute to changes in rolling and yawing moments, especially in the event that ice only accretes on one half of the wing. The exact amount of degradation, whether it is a change in side-force, rolling moment, or yawing moment depends on both the aircraft configuration and the particular derivative in question.

The percentage of degradation for each derivative of an evenly iced aircraft is imbedded within the MATLAB program that dimensionalizes the values calculated by AAA. Each of these dimensionalized counterparts of the derivatives is multiplied by an icing factor, f_{ice}, causing the derivative in question to become less stable. For example, the modification for C_{l_β} is

$$L_{\beta_{iced}} = \frac{\bar{q}Sb(1 + f_{ice})C_{l_\beta}}{I_{xx}} \tag{8}$$

such that static stability is reduced as C_{l_β} decreases. In this case an f_{ice} value of -0.10 is a degradation factor, meaning that C_{l_β} becomes less stable by 10%, based on data from the DeHavilland Twin Otter [4]. For the numerical examples these degradation factors are assumed to be the worst case scenario for icing on the Cessna 208B.

Eq. (8) generalizes the terms first presented in Eq. (1). For the purposes of this research f_{ice} represents the term $\eta_{ice}k'_{C_A}$. The actual parameterization of the terms η_{ice} and k'_{C_A} is beyond the scope of this paper, but is being addressed by other researchers. Instead, f_{ice} for each pertinent derivative is calculated from flight test data of the DeHavilland Twin Otter in both clean and icing conditions, as detailed in Ref. [4]. Since comprehensive icing data is not readily available for the Cessna 208B, applying icing data obtained from the DeHavilland Twin Otter does not fully represent what actually occurs in icing conditions. However, the simulated dynamic responses and performance are consistent with the limited scope and objectives of this research. Values of f_{ice} are presented in Table 1.

Please cite this article in press as: A. Lampton, J. Valasek, Prediction of icing effects on the lateral/directional stability and control of light airplanes, Aerospace Science and Technology (2011), doi:10.1016/j.ast.2011.08.005

Table 1
Change in stability and control derivatives due to icing [4].

Derivative	Clean value	f_{ice}
$-\Delta C_{L_0}$	0.26	0
$\Delta(-C_{L_\alpha} - C_{D_1})$	−4.53	−0.10
$-\Delta C_{L_q}$	10.27	−0.012
$-\Delta C_{L_{\delta_e}}$	0.54	−0.095
ΔC_{m_0}	0.10	0
ΔC_{m_α}	−0.78	−0.099
ΔC_{m_q}	−28.95	−0.035
$\Delta C_{m_{\delta_e}}$	−1.61	−0.10
ΔC_{Y_β}	−1.04	−0.20
$\Delta C_{Y_{\delta_r}}$	0.23	−0.08
ΔC_{l_β}	−0.10	−0.10
ΔC_{l_p}	−0.59	−0.10
$\Delta C_{l_{\delta_a}}$	0.15	−0.10
$\Delta C_{l_{\delta_r}}$	0.02	−0.08
ΔC_{n_β}	0.10	−0.20
ΔC_{n_r}	−0.20	−0.061
$\Delta C_{n_{\delta_a}}$	−0.01	−0.083

To analyze how the flight dynamics and performance change with ice accretion severity, additional factors are included in the calculation of the iced derivatives to represent various levels of severity. For example, the nominal f_{ice} degradation factor for C_{l_β} is −0.10, as stated above. By applying a coefficient or multiplier to f_{ice} in Eq. (8), the severity of the icing condition on the Cessna 208B can be manipulated. The multiplier can range from 0, representing a nominal or no ice condition, to 1, representing a worst case scenario icing condition. Similarly, if only mild icing is of interest, then f_{ice} may only be multiplied by 0.2, as shown in the following equation

$$L_{\beta_{iced}} = \frac{\bar{q}Sb(1 + 0.2 * f_{ice})C_{l_\beta}}{I_{xx}} \tag{9}$$

For the particular example shown, $0.2 f_{ice} = 0.2(-0.10) = -0.02$, which means that for "mild" ice C_{l_β} becomes less stable by 2%. This additional severity factor allows for increased versatility in examining possible effects icing has on the flight dynamics and performance of the airplane in question.

4.1. Asymmetric icing effects

Predicting the extent and severity of ice accretion prior to encountering icing conditions can be difficult due to its dependence on the configuration of the aircraft and numerous atmospheric conditions: an aircraft may be easily affected by even the smallest amount of ice, or it may be able to stay in flight without any adverse effects with very severe icing. In addition, an aircraft does not necessarily have to accumulate ice evenly between lifting surfaces or between wing halves. Some aircrafts tend to have a wing-icing problem only, others a horizontal tail icing problem, and still others do in fact accumulate ice fairly evenly between lifting surfaces. It is assumed here that the effects of distributed icing (different levels of ice on the wing and horizontal tail) appear as changes in the lift force and drag force of a given lifting surface, such as a wing or a horizontal tail. Before adding the icing effect to wing, tail, or wing half, an analysis is performed to determine the relative distribution of lift and drag between the wing-fuselage and the horizontal tail.

If ice is added to only the right half of the wing the method of applying icing factors to derivatives as described above no longer applies. In this case differences in lift and drag between the clean left wing and iced right wing will be used to determine induced rolling and yawing moments due to ice and integrated in to the state-space model described in previous sections.

This analysis is performed using trim values at 15,000 ft. Starting with the relation for total airplane lift coefficient and solving for lift coefficient of the horizontal tail. The full analysis can be found in Refs. [13] and [11]. The results of the analysis are that the horizontal tail generates approximately 20% of the lift that the wing-fuselage generates. Although drag data was not available, drag data for a similar aircraft configuration were used to provide a sanity check on the lift ratio above. Horizontal tail drag is also in the approximate proportion of 20% of the drag of the wing. This proportion means that rather than calculating the dimensionalized derivative for the whole airplane and applying f_{ice} as in (8), each derivative is split into two components that are then added together using component buildup. This split allows for a separate icing factor to be applied to the lift and drag contribution of the wing and the lift and drag contribution of the horizontal tail.

The next challenge is to calculate the change in lift and drag if ice accumulates on the right half of the wing only and the resulting rolling and yawing moments. Such a phenomenon is possible should the de-icing mechanism on only one wing half fail. The right half of the wing is chosen because the resulting differences in lift and drag between the two wing halves result in positive lateral/directional moments. The component buildup method is used employing the lifting surface asymmetry described above. The percent due solely to the wing is then halved for both the lift and drag equations. Icing factors are then applied, and the iced lift or iced drag is then subtracted from the clean lift and drag equations, as seen in Eq. (10) where the "ice" subscript denotes the right wing with ice applied, and the Δ indicates the difference between left and right wing halves.

$$\begin{aligned} \Delta C_{L_{ice}} &= \frac{1}{2}C_{L_{ice}} - \frac{1}{2}C_L \\ \Delta C_{D_{ice}} &= \frac{1}{2}C_D - \frac{1}{2}C_{D_{ice}} \end{aligned} \tag{10}$$

The difference in lift coefficient and drag coefficient are then dimensionalized as induced moment due to ice accretions by Eqs. (11) and (12) where d_{mgc} denotes the distance along the body X-axis from the mean geometric chord to the airplane centerline.

$$\Delta L_{ice} = \frac{\Delta C_{L_{ice}} \bar{q} S d_{mgc}}{I_{xx}} \tag{11}$$

$$\Delta N_{ice} = \frac{\Delta C_{D_{ice}} \bar{q} S d_{mgc}}{I_{zz}} \tag{12}$$

These induced moments are then integrated into the state-space equations described in previous sections by adding a disturbance term to the state-space formulation as seen in Eq. (13).

$$\dot{\boldsymbol{X}} = E^{-1}A\boldsymbol{X} + E^{-1}B\boldsymbol{U} + G\boldsymbol{W} \tag{13}$$

The disturbance term encompassing the induced moments due to ice accretion is represented by Eq. (14)

$$G\boldsymbol{W} = \begin{bmatrix} 0 & 0 \\ 0 & 0 \\ 0 & 0 \\ 0 & 0 \\ 0 & 0 \\ \Delta L_{ice} & 0 \\ 0 & \Delta N_{ice} \\ 0 & 0 \\ 0 & 0 \end{bmatrix} \begin{bmatrix} 1 \\ 1 \end{bmatrix} \tag{14}$$

where $\boldsymbol{W}$ corresponds to a constant step disturbance. To remain within the scope of this research, the induced moments are calculated for the first time step and held constant from then on, thus G is time invariant.

Please cite this article in press as: A. Lampton, J. Valasek, Prediction of icing effects on the lateral/directional stability and control of light airplanes, Aerospace Science and Technology (2011), doi:10.1016/j.ast.2011.08.005

Table 2
Flight and trim conditions for Cases 1–2.

Altitude (ft)	Airspeed (kts)	Dynamic pressure (lbs/ft^2)	Weight (lbs)	c.g. ($\bar{c}$)	α_1°	β_1°	$\delta_{a_1}^\circ$	$\delta_{r_1}^\circ$
15000	135	35.219	8402	0.289	5.51	0.13	0.18	−0.95

5. Simulation validation and verification

To validate the mathematics and physics of the airplane model and simulation, a series of standard maneuvers were performed to determine if the airplane model responds correctly and consistently to control inputs for a conventional airplane configuration with conventional controls. The results are reported in Refs. [12] and [11]. Four verification maneuvers were performed and compared to flight test data, to ensure that the simulation accurately represents a Cessna 208B Super Cargomaster. Flight test data was available for only a limited set of maneuvers, from which the verification maneuvers were selected. For brevity, only one lateral/directional maneuver is reproduced here. The maneuver is an aileron singlet, which excites the roll mode and verifies the lateral/directional dynamical model. These results are also reported in Refs. [12] and [11]. The results of the validation and verification maneuvers show that the lateral/directional model is judged to be acceptable as an accurate representation of the aircraft, within the limitations and accuracies of the methods used to construct the model.

6. Numerical examples

The simulation was used to evaluate several lateral/directional control inputs uneven icing scenarios for the purpose of determining the change in both dynamic response and performance due to various levels of ice accretion. One maneuver consisting of a rudder triplet followed closely by an aileron doublet and one case of ice on the right half of the wing only are presented to demonstrate the prediction of icing effects on aircraft states and parameters such as roll rate, yaw rate, and sideslip angle. The data presented in Table 1 represents mixed icing conditions [4]. These are the degradation factors that are applied to the stability and control derivatives shown in Eq. (8), and they indicate how much the lateral stability decreases for each derivative in the case of evenly accreted ice and the whole aircraft, and how much lift decreases and drag increases for the case of uneven accretion of ice on the right half of the wing. Subtracting each percentage from unity and applying it to the derivative indicated will effectively modify the aircraft model for icing. In addition, an increase of 15% was applied to the total drag, based on data obtained for the Twin Otter that shows an increase in drag of anywhere from 5% to ∼ 30% [4,5]. For the purpose of direct comparison, weight and airspeed are the same for each case, shown in Table 2.

6.1. Case 1: Rudder–aileron maneuver, fully iced configuration

This case investigates a parameter identification type maneuver consisting of a rudder 3–1–2 triplet followed closely by an aileron doublet and tracked for a period of 50 s. This example represents a configuration with evenly distributed amounts of mild ice accretions on both the wing and horizontal tail as well as between wing halves. For Case 1 “fully iced” means that 100% of the degradation factors listed in Table 1 are applied to their respective stability and control derivatives. This is effectively the “worst-case” scenario for an evenly iced aircraft.

Fig. 2 shows that the aileron doublet follows within 5 s of the rudder triplet and that bother the clean and iced aircraft are subjected to the same control inputs. The aircraft is close to trim for the cruise condition, which allows the differences between the clean and iced configurations during the maneuver to be easily seen without undue oscillations.

The effect of the “worst-case” scenario icing as shown in Fig. 2 demonstrates one of the major hazards of an iced aircraft: it does not respond to pilot commands in the same manner as a clean aircraft. Though the effect of ice is not extreme, differences between the iced and non-iced configurations do appear. The roll rate and pitch rate time histories of Fig. 2 show that the iced configuration “wobbles” more than the non-iced configuration. There is a maximum difference 25% and 20% for the roll rate and yaw rate, respectively, between the configurations. Also supported here are maximum differences in the sideslip angle, heading angle, and roll attitude angle on the order of 10%. However, despite these differences the iced aircraft returns trim, which suggests that it is still inherently stable.

6.2. Case 2: Uneven asymmetric icing, fully iced configuration

This case represents a “worst-case” scenario: an aircraft with one half of the wing fully accreted by ice. The full factors listed in Table 1 are applied to the model. This maneuver also consists of allowing the aircraft to respond to the ice induced lateral/directional moments and noting the roll-off tendencies of the iced aircraft.

Fig. 3 shows that the time histories for this “fully developed” ice accretion case indicate differences between the clean configuration and the fully iced configuration are much more pronounced here in Case 2. The aircraft has become unstable as shown in Fig. 3 as all of the states diverge. Numerical results show that roll rate and yaw rate have increased 600 and 210 deg/s, respectively. Sideslip angle has increases to an extreme value of −100 degrees in only 5 s. Consistent with these results are a roll attitude angle of over 650 degrees and a heading angle of 300 degrees. Due to the linear models used herein, these numerical results are beyond the linear range and thus are not an accurate representation of the response of a full nonlinear six degree-of-freedom model or the aircraft itself. However, they do show that asymmetric icing leads to instability and loss of control and that this approach can be used to predict that a loss of control will occur. Though the response is outside the linear range of the model, it is helpful to quantify the response using the time-to-double, which is 0.25 s for this case. More accurate and computationally intensive methods are necessary to investigate exactly how the aircraft will respond once beyond the linear range.

7. Conclusions and recommendations for further research

An analysis method using flight data, wind tunnel data, and the United States Air Force Data Compendium was developed to create a basic but reasonably detailed and accurate simulation model that accounts for the effects of ice accretion on light aircraft. The component build-up method was used to implement icing effects one half of the wing alone and combined wing and horizontal tail using icing data on similar light aircraft. The icing data used was obtained empirically, and modified for the aircraft configuration considered. The scope of the present work was limited to the lateral/directional axis, where the some detrimental icing effects are experienced. A linear time invariant, state-space model of the lateral/directional model of a representative light aircraft was

Please cite this article in press as: A. Lampton, J. Valasek, Prediction of icing effects on the lateral/directional stability and control of light airplanes, Aerospace Science and Technology (2011), doi:10.1016/j.ast.2011.08.005

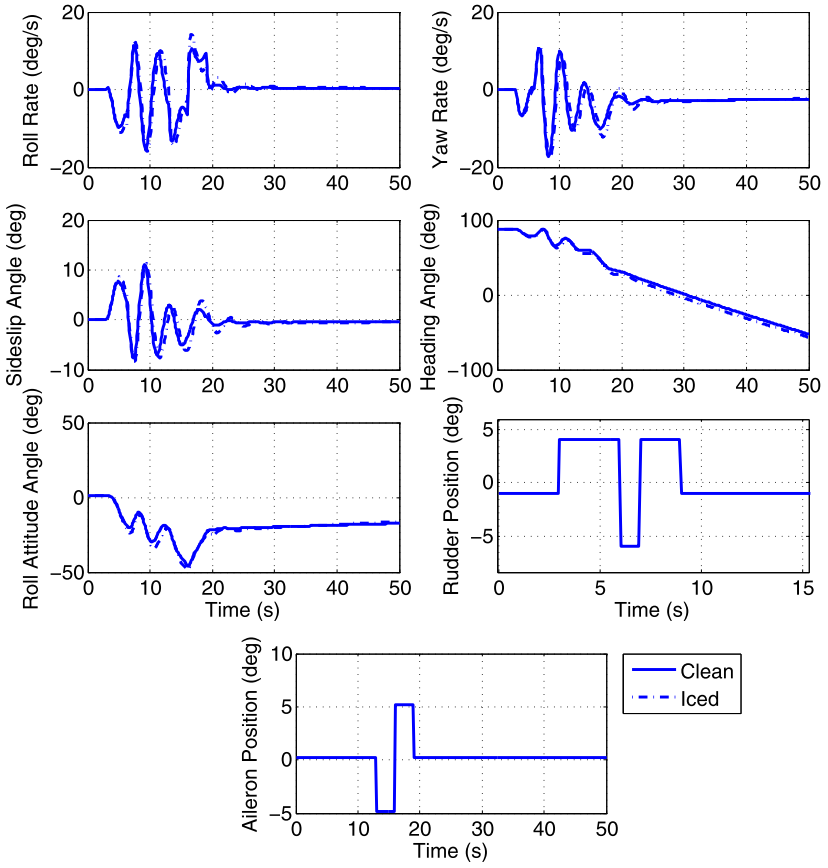

Fig. 2. Case 1 time histories of clean and fully iced aircraft for parameter identification maneuver.

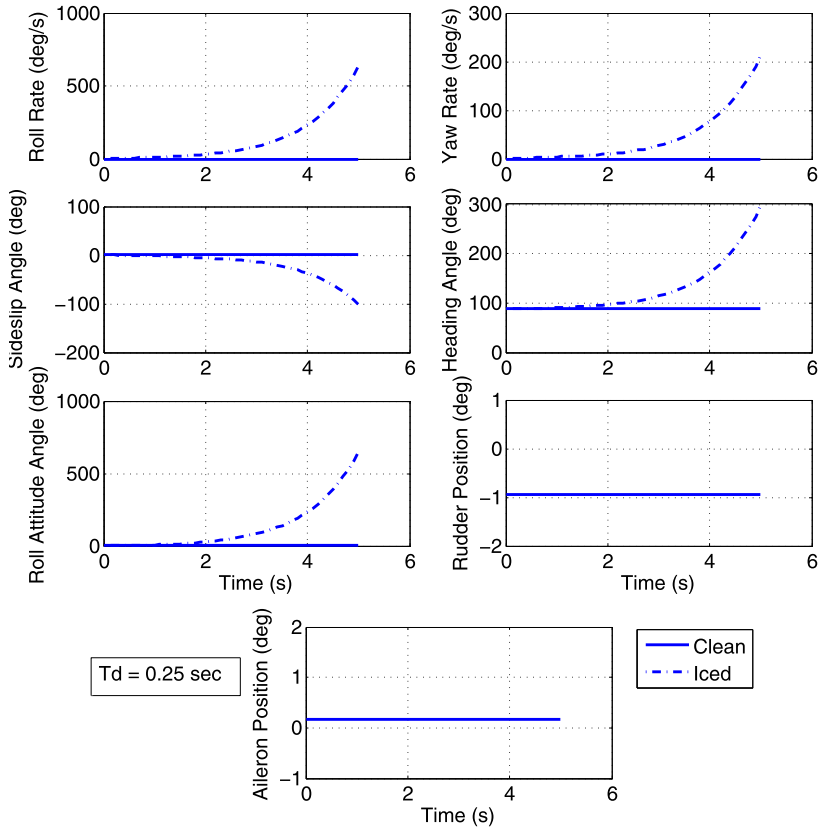

Fig. 3. Case 3 time histories of clean aircraft and aircraft with right wing half fully iced.

Please cite this article in press as: A. Lampton, J. Valasek, Prediction of icing effects on the lateral/directional stability and control of light airplanes, Aerospace Science and Technology (2011), doi:10.1016/j.ast.2011.08.005

developed, and used for non-real-time simulation to evaluate icing effects on stability and control characteristics, in addition to effects on roll-off tendencies. Validation of the simulation model was conducted using several basic maneuvers, and verification was conducted using flight test data for the same aircraft as the simulation. Numerical examples consisting of a parameter identification type maneuver and two uneven icing roll-off assessments in various levels of icing were evaluated, and based on the results presented in the paper the following conclusions are drawn:

1. The linear state-space model representation, discrete simulation model, and inclusion of simplified icing effects appear to be an adequate tool for basic icing dynamics and performance analysis for the maneuvers investigated. Verification results to flight data showed good agreement for the maneuvers investigated here, and only relatively simple data was needed to construct the models.
2. Qualitatively, from the simulation results evenly distributed ice caused the aircraft to become less stable, but the evenly iced aircraft remains inherently stable for the type of maneuver investigated.
3. For the uneven accretion comparisons of iced aircraft to clean aircraft allowing the iced aircraft to respond to ice induced moments without any control inputs, simulation results showed an adverse affect on lateral/directional stability:
   a. The 100% iced right wing half configuration experienced the following within 5 s:
      i. First-order departure from controlled flight,
      ii. Time-to-double = 0.25 s.

Acknowledgements

This research is funded by the Aeronautical and Educational Services Company, under grant number C05-00356. The technical monitor is Dr. Donald T. Ward. The authors gratefully acknowledge this support.

Appendix A. Linear state-space models of clean Cessna 208B Super Cargomaster

$$\begin{bmatrix} \dot{\beta} \\ \dot{p} \\ \dot{r} \\ \dot{\phi} \\ \dot{\psi} \end{bmatrix} = \begin{bmatrix} -0.17 & -0.0014 & -0.99 & 0.14 & 0 \\ -5.96 & -4.10 & 0.77 & 0 & 0 \\ 2.16 & -0.19 & -0.52 & 0 & 0 \\ 0 & 1 & 0.10 & 0 & 0 \\ 0 & 0 & 1.00 & 0 & 0 \end{bmatrix} \begin{bmatrix} \beta \\ p \\ r \\ \phi \\ \psi \end{bmatrix} + \begin{bmatrix} 0 & 0.04 \\ 8.99 & 1.10 \\ -0.07 & -2.63 \\ 0 & 0 \\ 0 & 0 \end{bmatrix} \begin{bmatrix} \delta_a \\ \delta_r \end{bmatrix}$$

References

[1] Advanced Aircraft Analysis, Design, Analysis, and Research Corporation, 2003.
[2] Anonymous, Cessna Aircraft Company Model 208 Maintenance Manual, April 1996.
[3] M. Bragg, Aircraft aerodynamic effects due to large droplet ice accretions, No. AIAA-96-0932, Reno, NV, January 1996.
[4] M. Bragg, T. Hutchison, J. Merret, R. Oltman, D. Pokhariyal, Effect of ice accretion on aircraft flight dynamics, No. AIAA-2000-0360, Reno, NV, January 2000.
[5] M. Bragg, S. Lee, Aircraft icing flight dynamics model for twin otter aircraft, Tech. rep., Final Technical Report 10817/1329/TTM to Systems Technology, Inc., Hawthorne, CA, October 2000.
[6] M. Bragg, W. Perkins, N. Sarter, T. Basar, P. Voulgaris, H. Gurbacki, J. Melody, S. McCray, An interdisciplinary approach to inflight aircraft icing safety, No. AIAA-98-0095, Reno, NV, January 1998.
[7] A. Broeren, H.E. Addy Jr., M. Bragg, Effect of intercycle ice accretions on airfoil performance, Journal of Aircraft 41 (1) (2004) 165–174.
[8] A. Broeren, H.E. Addy Jr., M. Bragg, Flowfield measurements about an airfoil with leading-edge ice shapes, No. AIAA-2004-0559, Reno, NV, January 2004.
[9] A. Broeren, M. Bragg, Effect of airfoil geometry on performance with simulated intercycle ice accretions, Journal of Aircraft 42 (1) (2005) 121–130.
[10] H. Gurbacki, M. Bragg, Unsteady aerodynamic measurements on an iced airfoil, No. AIAA-2002-0241, Reno, NV, January 2002.
[11] A. Lampton, J. Valasek, Prediction of icing effects on the coupled dynamic response of light airplanes, Journal of Guidance, Control, and Dynamics 30 (3) (2008) 722–732.
[12] A. Lampton, J. Valasek, Prediction of icing effects on the lateral/directional stability and control light airplanes, No. AIAA-2006-6487, Keystone, CO, August 2006.
[13] A. Lampton, J. Valasek, Prediction of icing effects on the dynamical response of light airplanes, Journal of Guidance, Control, and Dynamics 30 (3) (May–June 2007) 722–732.
[14] S. Lee, M. Bragg, Experimental investigation of simulated large-droplet ice shapes on airfoil aerodynamics, Journal of Aircraft 36 (5) (1999) 844–850.
[15] S. Lee, M.B. Bragg, Investigation of factors affecting iced-airfoil aerodynamics, Journal of Aircraft 40 (3) (2003) 499–508.
[16] B. Lu, M. Bragg, Airfoil drag measurement with simulated leading-edge ice using the wake survey method, No. AIAA-2003-1094, Reno, NV, January 2003.
[17] J.W. Melody, T. Basar, W.R. Perkins, P.G. Voulgaris, Parameter identification for inflight detection and characterization of aircraft icing, Control Engineering Practice 8 (9) (2000) 985–1001.
[18] T. Ratvasky, T. Ranaudo, Icing effects on aircraft stability and control determined from flight data, No. AIAA-93-0398, Reno, NV, January 1993.
[19] M. Rauw, FDC 1.3 – A SIMULINK toolbox for flight dynamics and control analysis, Website: http://www.mathworks.com/matlabcentral/fileexchange, 1998.
[20] A. Reehorst, J. Chung, M. Potapczuk, Y. Choo, Study of icing effects on performance and controllability of an accident aircraft, Journal of Aircraft 37 (2) (2000) 253–259.
[21] V. Sharma, P. Voulgaris, E. Frazzoli, Aircraft autopilot analysis and envelope protection for operation under icing conditions, Journal of Guidance, Control, and Dynamics 27 (3) (2004) 454–465.
[22] K. Sibilski, M. Lasek, E. Ladyzynska-Kozdras, J. Maryniak, Aircraft climbing flight dynamics with simulated ice accretion, No. AIAA-2004-4948, Providence, RI, August 2004.
[23] E. Whalen, M. Bragg, Aircraft characterization in icing using flight-test data, Journal of Aircraft 42 (3) (2005) 792–794.

Please cite this article in press as: A. Lampton, J. Valasek, Prediction of icing effects on the lateral/directional stability and control of light airplanes, Aerospace Science and Technology (2011), doi:10.1016/j.ast.2011.08.005